

Preneoplastic Changes in Ovarian Tissues

Molly A. Brewer, D.V.M., M.D., M.S., James Ranger-Moore, Ph.D.,
Mark H. Greene, M.D., David S. Alberts, M.D., Yun Liu, M.D., Hubert G. Bartels,
M.S.I.E., Amy C. Baruch, M.D., and Peter H. Bartels, Ph.D., F.I.A.C.(hon)

OBJECTIVE: To test whether histologically normal epithelium within ovarian inclusion cysts and stroma exhibit changes in nuclear chromatin pattern that indicate the presence of occult ovarian lesions.

STUDY DESIGN: Ovaries were collected from 10 low-risk women, from 7 high-risk women and from 3 women with ovarian cancer. Histologic sections were cut at 5 μ m and hematoxylin and eosin stained. High-resolution images were recorded from the epithelium lining inclusion cysts and from the underlying stroma of ovaries from these 20 subjects. A total of 2,860 epithelial nuclei and 3,610 stromal nuclei were recorded. Karyometric features and nuclear abnormality were computed. Discriminant analyses and unsupervised learning algorithms de-

finied deviations from normal that were designated "above threshold" and used to compute average nuclear abnormality of a second nuclear phenotype.

RESULTS: Histologically normal epithelium from inclusion cysts of ovaries harboring a malignant lesion was shown to exhibit changes in the nuclear chromatin pattern that were statistically significant using quantitative image analysis procedures. Similar changes were seen in the inclusion cyst epithelia of high-risk ovaries. A sub-population of cells representing a new phenotype was detected in the underlying stroma of women harboring a malignant ovarian lesion and in women at high risk of ovarian cancer.

CONCLUSION: The karyometric changes observed in

From the Arizona Cancer Center; College of Public Health; Optical Sciences Center; College of Medicine, Division of Pathology; Biomedical Engineering; and Division of Gynecologic Oncology, Department of Obstetrics and Gynecology, University of Arizona, Tucson, Arizona, and Clinical Genetics Branch, Division of Cancer Epidemiology and Genetics, National Cancer Institute, National Institutes of Health, Bethesda, Maryland, U.S.A.

Dr. Brewer is Associate Professor, Arizona Cancer Center, College of Medicine, Biomedical Engineering and Department of Obstetrics and Gynecology, University of Arizona.

Dr. Ranger-Moore is Assistant Professor, Arizona Cancer Center and College of Public Health, University of Arizona.

Dr. Greene is Chief, Clinical Genetics Branch, Division of Cancer Epidemiology and Genetics, National Cancer Institute, National Institutes of Health.

Dr. Alberts is Regent's Professor of Medicine, Pharmacology and Public Health and Director of Cancer Prevention and Control.

Dr. Liu is Research Specialist, Sr., Arizona Cancer Center.

Mr. Bartels is Systems Programmer, Sr., Optical Sciences Center, University of Arizona.

Dr. Baruch is Clinical Assistant, College of Medicine, Department of Pathology, University of Arizona.

Dr. Bartels is Professor Emeritus, Arizona Cancer Center and Optical Sciences Center, University of Arizona.

Address reprint requests to: Molly A. Brewer, D.V.M., M.D., M.S., Division of Gynecologic Oncology, Department of Obstetrics and Gynecology, Arizona Cancer Center, Room 1968G, 1515 North Campbell Avenue, Tucson, Arizona 85724-5024 (mbrewer@azcc.arizona.edu).

Supported in part by grants from the National Institutes of Health, National Cancer Institute, CA 53877-13, to P.H.B., and CA 27502-22S1, to D.A. Additional support has come from a University Physicians/University Medical Experimental Research for Clinical Care grant, University of Arizona.

The contents of this paper are solely the responsibility of the authors and do not necessarily represent the official view of the National Cancer Institute.

Financial Disclosure: The authors have no connection to any companies or products mentioned in this article.

the epithelia lining inclusion cysts and in the underlying stroma of ovaries either with ovarian cancer or at high risk of ovarian cancer suggest the presence of preneoplastic changes in histologically normal tissue. (Analyst Quant Cytol Histol 2004;26:207–216)

Keywords: ovarian neoplasms, ovarian cancer, karyometry, stromal cells, ovarian inclusion cysts.

Ovarian cancer has the highest mortality of all gynecologic cancers; 70% of women with it die of the disease within 5 years. The absence of information on precursor lesions represents a barrier to early cancer detection and to development of therapeutic agents that might alter the potential for developing a malignancy. Although the overall cumulative lifetime risk of ovarian cancer is relatively low (1.5–1.7%), there are subgroups of women with a moderately or significantly increased risk of ovarian cancer who have a higher disease incidence than does the normal population.¹ Women with a family history suggestive of hereditary breast/ovarian cancer syndrome are at exceedingly high risk, with lifetime probabilities of developing ovarian cancer ranging from 16% to 40%.² Such women would benefit from a better understanding of the early changes that precede the onset of ovarian cancer to facilitate cancer prevention and early detection strategies.

In a preceding exploratory study,³ nuclei from histologically normal appearing ovarian surface epithelium were subjected to karyometric analyses. That study was undertaken to test the hypotheses that (1) histologically normal appearing ovarian surface epithelium from cases harboring an ovarian lesion might exhibit so-called malignancy associated changes⁴ that were not visually perceived but that were computationally detectable and that (2) similar changes might be detectable in the ovarian surface epithelium derived from ovaries without cancer that are obtained from patients at high risk of developing ovarian cancer.

Both hypotheses were confirmed. Karyometry clearly revealed statistically significant changes in the nuclei from both types of surface epithelium but not in tissue derived from the normal ovaries of normal-risk women. The observed changes were referred to as “preneoplastic changes” because no visually apparent evidence of neoplastic tissue changes was seen, and the karyometric characteristics were similar to those seen in other premalignant and malignant lesions.^{5–15}

In the current study, histopathologic sections prepared from the same material as in the original exploratory study were analyzed for evidence of changes in nuclear phenotype in the epithelial lining of ovarian inclusion cysts and in the underlying stroma of these ovaries.

Materials and Methods

The low-risk group was composed of women undergoing incidental oophorectomy for benign indications and who lacked a familial predisposition to ovarian cancer (estimated lifetime risk, 1.4–1.7%). The high-risk group was composed of women with a family or personal history of breast and/or ovarian cancer, which implied a higher risk of developing ovarian cancer (>5% lifetime risk). This group included a small percentage of patients who had undergone genetic testing; those that carry a germline mutation will have a much higher probability of developing ovarian cancer than other patients (BRCA1, 40–60% lifetime risk; BRCA2, 8–10% lifetime risk). Patients signed a University of Arizona institutional review board–approved consent form. Ovaries were harvested at the time of laparoscopic or open oophorectomy.

The clinical materials for this study consisted of hematoxylin and eosin (H&E)–stained histopathologic sections from: (1) 10 cases with normal ovaries from normal-risk women, free of any premalignant or malignant lesion, in which 1,336 nuclei were analyzed in the epithelium of inclusion cysts; (2) 7 cases of histologically normal appearing ovaries also free of any premalignant or malignant ovarian lesion but from patients considered at increased risk of ovarian cancer, in which 949 nuclei were measured in the epithelium of inclusion cysts; and (3) 3 cases of ovarian cancer, in which 575 nuclei in histologically normal appearing epithelium in inclusion cysts were recorded. For measurements in the ovarian stroma, 1,784, 1,411 and 415 nuclei, respectively, were analyzed.

The following abbreviation dyads are used to denote the data sets: “norm/norm”: normal histology/normal risk subjects; “norm/HR”: normal histology/high-risk subjects; and “norm/ca”: normal histology/ovaries with cancer. Thus, all nuclei were measured in histologically normal appearing tissue. In addition, the suffix “CYST” was added to distinguish the data derived from the epithelial lining of ovarian inclusion cyst sets from those recorded within surface epithelium in the preceding exploratory study, which are denoted by the suffix

Table I Seven Karyometric Features Comparing Cyst Epithelium from Normal Patients and from Cancer Patients

Variable	norm/norm-CYST	norm/ca-CYST
Total OD	0.268	0.338
Nuclear area	15.2	17.3
Run length nonuniformity	4.42	5.16
Pixel OD heterogeneity	0.425	0.373
Pixel OD homogeneity	0.574	0.627
Mean pixel OD	45.57	51.12
No. of "grey" pixels in nucleus	584	724

"SE." Data recorded from stromal nuclei are denoted by the suffix "STR."

Data recording was done on a videomicrophotometer equipped with a 100:1 N.A. 1.40 planapochromatic oil immersion objective (Carl Zeiss, Oberkochen, Germany). The relay optics adjusted image sampling to 6 pixels per linear micron. Images were recorded on a Sony DXC 9000 3-CCD color camera (Sony, Melville, New York, U.S.A.). For maximum contrast in the H&E-stained sections only the red channel image was used for feature computation. Nuclei were segmented by a semiautomated procedure. Each recorded field was laser printed and each segmented nucleus identified for later reference. For each nucleus 93 karyometric features descriptive of the spatial and statistical distribution of the nuclear chromatin were computed. Feature descriptions and the computation of nu-

Table II Percentage of Second Phenotype of Surface Epithelium as Compared to Inclusion Cyst Epithelium

Diagnostic group % of abnormal nuclei	Surface epithelium (%)	Inclusion cyst epithelium (%)
norm/norm	10.8	25
norm/HR	25.4	24.3
norm/CA	57.4	50

clear and lesion signatures are described in previous publications.^{5,6,16}

Results

Measurements from Nuclei in the Epithelium Lining Inclusion Cysts

To identify characteristics that might distinguish nuclei from the norm/norm-CYST data set from nuclei of the norm/ca-CYST data sets, a Kruskal-Wallis test¹⁸ was done. It identified 48 karyometric features with differences at a significance level of $P < .005$. From this set of features 7 were selected from different feature blocks (such as pixel optical density (OD), histogram, co-occurrence matrix, run length features) that represent different aspects of karyometric abnormalities and subjected to a stepwise discriminant algorithm.

The feature values, averaged over all nuclei in the sample subsets norm/norm and norm/ca, showed significant differences for many of the features (Table I). All feature values are given in arbitrary, relative units per karyometric imaging convention.

The discriminant analysis showed the 2 data sets to be statistically significantly different. The absolute differences in feature mean values are not large, but the test for statistical significance was computed at a high-power level due to the large number of nuclei.

The analysis led to correct classification of 66% of nuclei. Figure 1 shows the discriminant function score distributions. There is a distinct shift for the nuclei from ovaries with coexisting cancer. The score distribution from the norm/norm-CYST data set exhibits noticeable dispersion. It does not display the typical peaked shape expected for a normal population of nuclei, as seen in the norm/norm SE data set reported earlier. The distribution also ex-

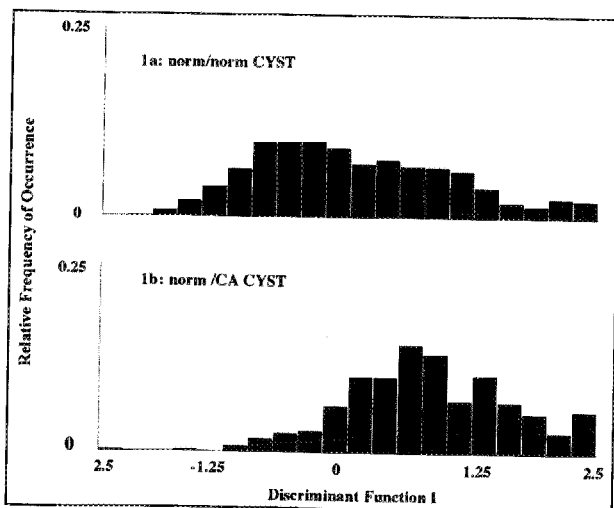


Figure 1 Distributions of discriminant function I scores for nuclei from inclusion cysts of normal ovaries and of ovaries from cases harboring ovarian cancer.

Table III Average Nuclear Abnormality

Variable	norm/norm	norm/HR	norm/ca
Nuclear abnormality	0.620	0.702	0.758

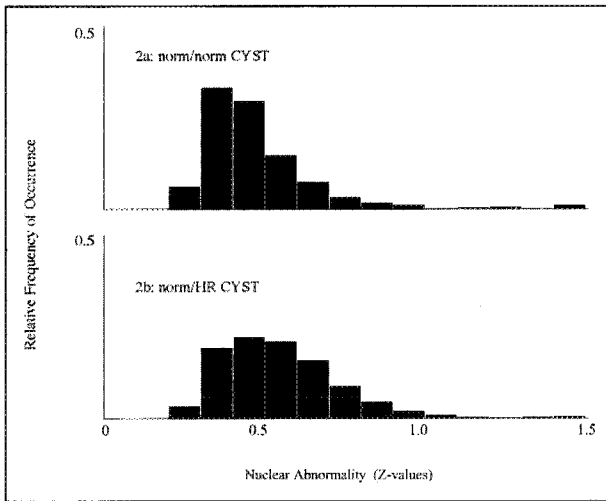


Figure 2 Distributions of nuclear abnormality values for nuclei from inclusion cysts of normal ovaries and nuclei from normal ovaries of cases at high risk for ovarian cancer.

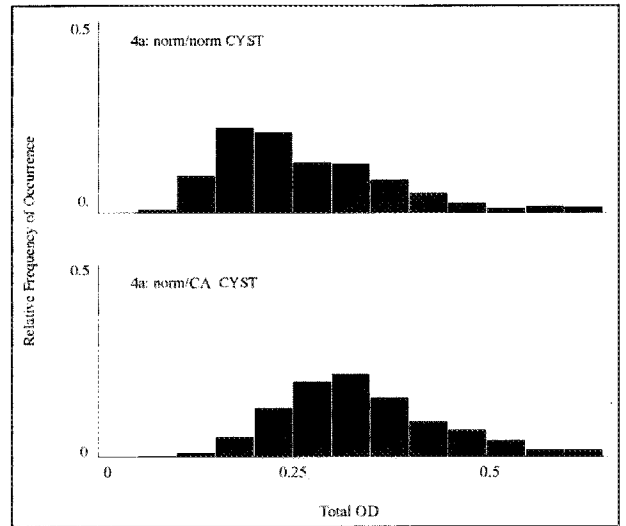


Figure 4 Distributions of total OD for nuclei from inclusion cysts of normal ovaries and ovaries harboring cancer.

tends further into the score range occupied by nuclei from the norm/ca CYST data set than seen in the corresponding data set from nuclei in the surface epithelium.

The differences attributable to the presence of the coexisting ovarian lesion find expression in higher discriminant function scores. Setting a threshold in the score distribution such that roughly 50% of the nuclei from the norm/ca data set fall above that

threshold, we found that 25% of the nuclei from the norm/norm-CYST data set fall into the higher value range. The measurements in nuclei from patients at high risk of developing ovarian cancer (norm/HR-CYST) show a distribution of discriminant function scores that is almost identical to that seen in the norm/norm-CYST data set, with 24.3% of nuclei exceeding the threshold, the same proportion seen in the norm/norm CYST data set.

The dispersion and shape of the score distributions from the norm/norm-CYST and the norm/HR-CYST data are very similar to the distributional characteristics of the norm/HR SE data and markedly different from those of the norm/norm SE data. This suggests that the epithelial nuclei of inclusion cysts, even in normal-risk women, may already be expressing karyometric abnormalities that are more typical of those seen in high-risk ovaries or ovaries that actually contain a malignancy. In that sense it may be that important differences exist between the nuclei of the ovarian surface epithelium and the nuclei in epithelia that

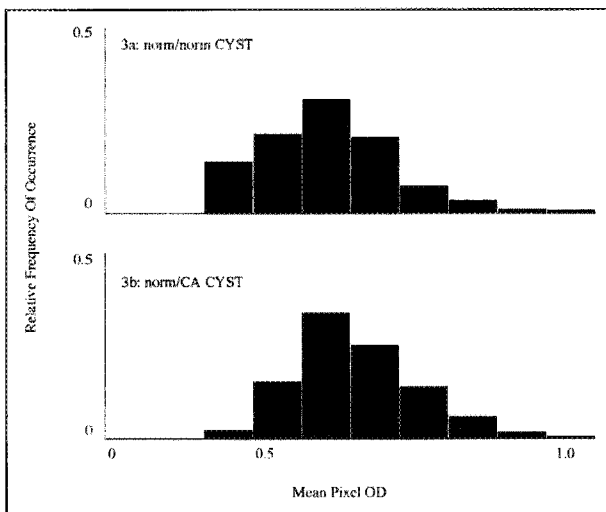


Figure 3 Distributions of mean staining density for nuclei from inclusion cysts of normal ovaries and ovaries harboring cancer.

Table IV Average Nuclear Abnormality

Diagnostic group	Average nuclear abnormality
norm/norm STR	0.456
norm/HR STR	0.525
norm/ca STR	0.574

Table V Seven Karyometric Features Comparing Stroma from Normal Patients and from Cancer Patients

Variable	norm/norm STR	norm/ca STR
Total OD	0.123	0.209
Relative nuclear area	6.71	10.39
Co-occurrence feature 3, 2	3.00	7.05
OD level nonuniformity	11.47	15.1
Run length nonuniformity	4.55	5.68
Run percentage	135.15	219.32
No. of "black" pixels in nucleus	88.6	141.5

line inclusion cysts, even in normal subjects.

Table II compares the proportions of nuclei resembling the 50% of nuclei expressing preneoplastic change in the norm/ca data sets.

The difference between 10% vs. 25% in the norm/norm-SE and the norm/norm-CYST data is significant at $P < .01$. The differences between the norm/HR and the norm/ca data sets from both the surface epithelium and the inclusion cyst epithelium are significant at the $P < .01$ level.¹⁷

Overall, there is a monotonic rise in the average nuclear abnormality for the subpopulations above the 50% threshold from the norm/norm-CYST data to the norm/ca CYST data (Table III).

Figure 2 shows the distribution of the nuclear abnormality for the norm/norm-CYST and the norm/HR-CYST data sets. There is a clear shift towards higher nuclear abnormality in the latter group.

There are several other karyometric features that display similar differences—e.g., the number of pixels with an average "grey" pixel OD value rise from 586 to 597 and to 720 in the same subsets.

Figure 3 shows the pixel OD histogram for the norm/norm-CYST and norm/ca-CYST data; it parallels the pattern seen in the surface epithelium data. Figure 4 shows the increase in total OD for nuclei from norm/norm-CYST and norm/ca-CYST.

Measurements in Stromal Nuclei

For each of the cases in which epithelial cells were

Table VI Classification Result for DF II of Stroma

Diagnostic group	Classification by DF II	
	norm/norm STR (%)	norm/ca STR (%)
Visual diagnosis		
norm/norm STR	78.5	21.5
norm/ca STR	24.1	75.9

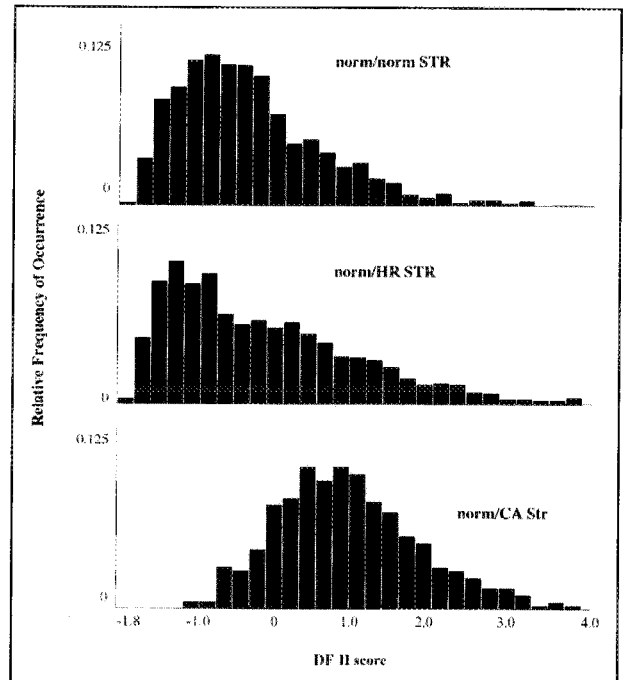


Figure 5 Distributions of DF II scores for nuclei from stroma of normal ovaries, normal ovaries from cases at high risk of developing ovarian cancer and ovaries from cases harboring cancer.

measured, measurements were also taken from nuclei in the underlying stroma. The objective was to test the hypothesis that the underlying stroma is not merely an inactive support medium but rather that stromal cells might be active participants in a preneoplastic process that eventuates in overt ovarian cancer.

The average stromal nuclear abnormality score shows a moderate rise from cases of normal ovaries to those from high-risk subjects to stroma from women with a malignant lesion (Table IV).

A Kruskal-Wallis test revealed numerous features with highly significant ($P < .005$) differences between the norm/norm-STR and the norm/ca-STR data sets. Table V provides a list of some of these features, with their mean values.

Table VII Mean Discriminant Function Score II of Stroma

Diagnostic group	Mean DF II score
norm/norm-STR	-0.230
norm/HR-STR	-0.046
norm/ca-STR	0.989

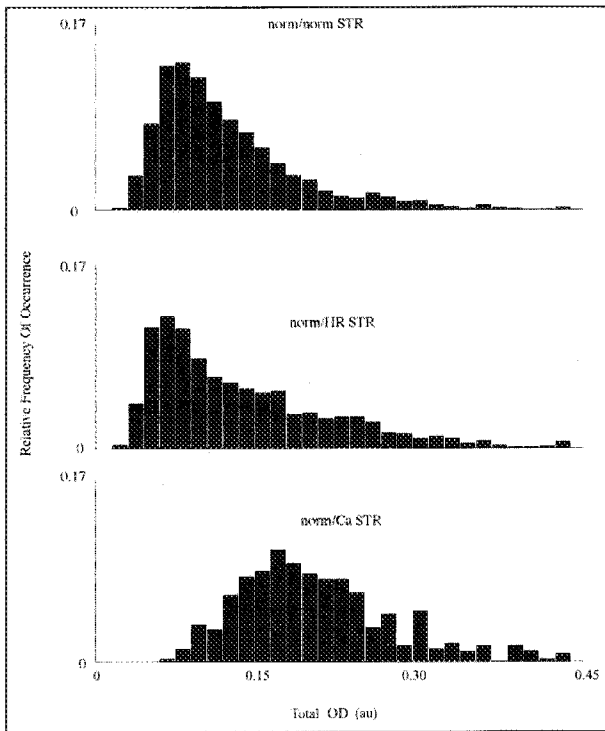


Figure 6 Distributions of total OD for nuclei from stroma of normal ovaries, normal ovaries from cases at high risk of developing ovarian cancer and ovaries from cases harboring cancer.

A discriminant analysis (DF II) resulted in the reduction of Wilks' lambda to .772, with relative nuclear area, total OD and run length nonuniformity the features with the greatest weights in the function. In normal-appearing stromal nuclei from normal ovaries, DF II correctly classified 78.5%. In normal-appearing stromal nuclei from ovaries with a lesion, DF II correctly classified 75.9%. Overall, classification based on DF II scores resulted in an average correct classification rate of 78.0%.

The classification matrix for nuclei is given in Table VI.

Figure 5 shows the distribution of discriminant function scores for the norm/norm STR, norm/HR STR and norm/ca STR data sets. The mean discriminant function scores are given in Table VII.

Figure 6 shows the distribution of total OD values for the 3 data sets. There is a steady shift towards higher values.

A bivariate plot of the data presented for the average nuclear abnormality (Table IV) and for the mean discriminant function II score (Table VII) is

shown in Figure 7. The confidence ellipses for the bivariate means are distinctly separate, with the mean from norm/HR-STR close to norm/norm-STR and the nuclei from norm/ca-STR widely separated, at higher nuclear abnormality and discriminant function II scores. While it is evident that statistically significant changes occur in the stromal nuclei when analyzed in the aggregate, these data do not speak to the issue of whether these changes affect all nuclei or only a subpopulation.

To test the set of 415 nuclei measured in the stroma of the norm/ca-STR data set, the set of features used in the discriminant function II was subjected to the nonsupervised learning algorithm, P-index.¹⁷ These features were total OD, nuclear area, run length nonuniformity and run percentage. The P-index algorithm formed 2 clusters, but the Beale statistic¹⁶ found them to be statistically not significantly different ($P = .72$). However, the Beale statistic in its assessment of statistical significance relies on the overlap of tolerance regions between clusters rather than the difference in cluster centroid locations. When subjected to a Kruskal-Wallis test, the 2 clusters were shown to have statistically highly significant differences for >20 karyometric features, at

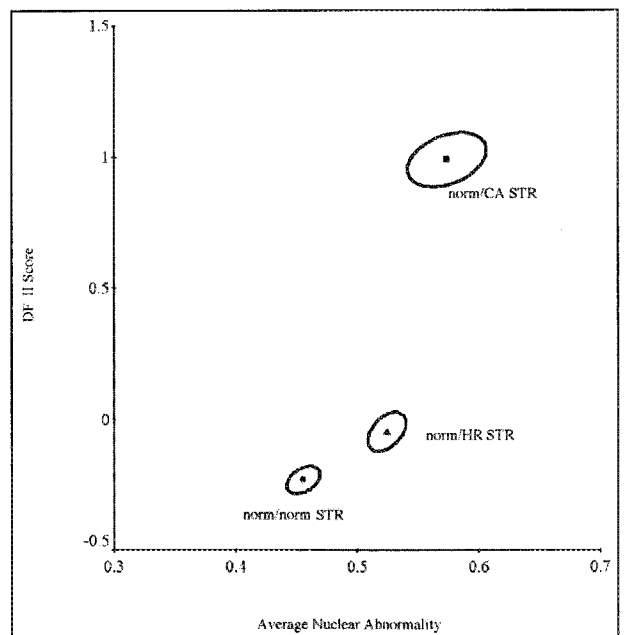


Figure 7 Progression curve, mean DF II score plotted vs. average nuclear abnormality for stromal nuclei from normal ovaries, from normal ovaries of cases at high risk of developing ovarian cancer and ovaries harboring cancer. Shown are the 95% confidence ellipses for the means.

Table VIII Classification Result of DF III

P-index assignment	DF III assignment (%)	
	Cluster 1	Cluster 2
Cluster 1	80.4	19.6
Cluster 2	4.3	95.7

For an average of 92.3% correct classification.

$P < .005$. Six of these features were subjected to a discriminant analysis (DF III), which resulted in a reduction of Wilks' lambda to .41, i.e., the 2 subpopulations were found to be separable by a selection of features more effective for this task than those used in the function DF II. The variance of pixel OD values, the nuclear area and the number of

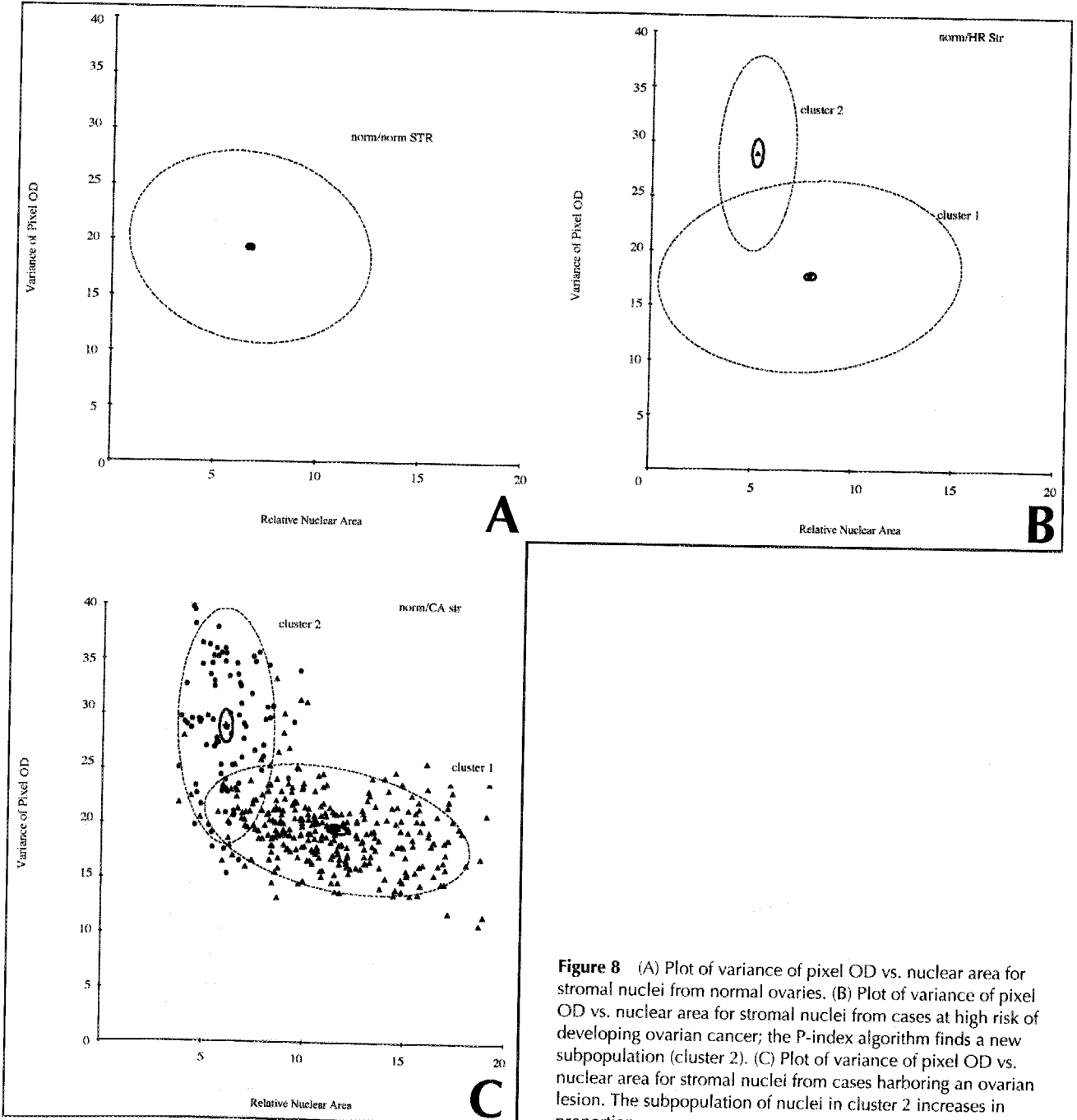


Figure 8 (A) Plot of variance of pixel OD vs. nuclear area for stromal nuclei from normal ovaries. (B) Plot of variance of pixel OD vs. nuclear area for stromal nuclei from cases at high risk of developing ovarian cancer; the P-index algorithm finds a new subpopulation (cluster 2). (C) Plot of variance of pixel OD vs. nuclear area for stromal nuclei from cases harboring an ovarian lesion. The subpopulation of nuclei in cluster 2 increases in proportion.

Table IX *New Subpopulation*

Diagnostic category	% Abnormal	No. of cells
norm/norm-STR	0.01	1/1,784
norm/HR-STR	6.3	88/1,411
norm/ca-STR	22.8	92/415

very dark pixels in a nucleus were given the greatest weights in the function DF III. The classification matrix is given in Table VIII.

Figure 8 shows bivariate plots of the subpopulations found in these data sets for the features nuclear area and variance of pixel OD. The norm/norm-STR data set is homogeneous, forming only cluster 1—i.e., nuclei at low pixel OD variance and with large nuclear area. The second, new subpopulation first appears in the norm/HR-stroma and is strongly represented in the stroma of ovaries harboring a malignant lesion (cluster 2), as seen in Figure 8.

Table IX shows the percentages of nuclei in the 2 subpopulations.

Figure 9 shows the distributions of pixel OD variance for the 3 data sets: norm/norm-STR, norm/HR-STR (cluster 2) and norm/ca-STR (cluster 2).

Figure 10 shows a plot of nuclear abnormality vs. discriminant function III score for the new subpopulation identified in norm/HR-STR and norm/ca-STR. It shows that the new subpopulations are not only similar but that the 95% confidence limits for the bivariate means overlap and that both differ significantly from the bivariate mean for norm/norm-STR stroma.

Discussion

The present study followed an effort aimed at searching for evidence of preneoplastic changes in ovarian surface epithelium. In our prior work, statistically significant changes were documented in the nuclei from histologically normal appearing epithelium of ovaries harboring a malignant lesion as well as in the epithelium of ovaries free of any such lesions but from patients at high risk of developing ovarian cancer. In these latter epithelia, a certain proportion of nuclei retain "normal" characteristics, whereas in the histologically normal epithelium from ovaries harboring a malignant lesion all nuclei exhibit deviations from normal.

The recorded changes in the nuclear chromatin pattern are similar to those observed in histologi-

cally normal appearing tissue of organs with coexisting premalignant or malignant lesions—e.g., in the bladder,⁹ uterine cervix,^{10,11} prostate,^{12,13} breast,¹⁵ thyroid¹⁷ and colon.¹⁸ One might consider these deviations from normal as representing intraepithelial lesions, or "ovarian intraepithelial neoplasia," but for the effect observed here, the term *preneoplastic lesion* seems preferable since there is no visual evidence using standard histologic techniques for examining neoplasia.

In the current study, image analysis of the previously reported specimens was extended to nuclei from epithelia within inclusion cysts and to nuclei within the underlying ovarian stroma. Again, clearly expressed preneoplastic changes similar to those previously reported in the surface epithelium were documented both in cellular compartments from patients at high risk of ovarian cancer and from ovaries harboring a malignant lesion.

The epithelium of inclusion cysts from normal ovaries from normal patients is more similar to the nuclei in inclusion cysts from patients at high risk of ovarian cancer. They are clearly different from the

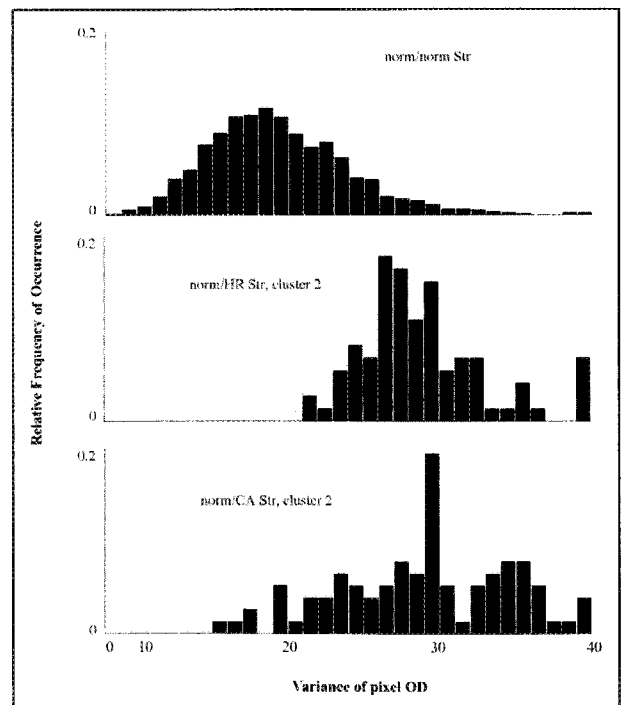


Figure 9 Distributions of variance of pixel OD values for stromal nuclei from normal ovaries and for the nuclei of cluster 2 in normal ovaries of cases at high risk of developing ovarian cancer and ovaries harboring a lesion.

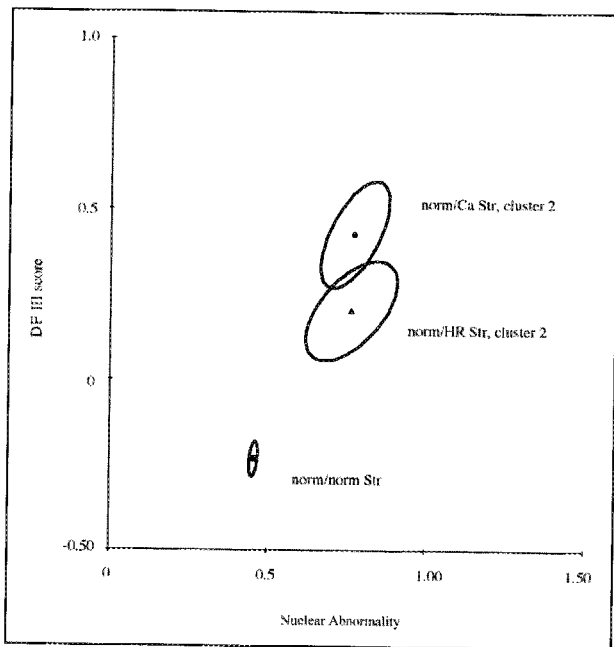


Figure 10 DF II scores plotted vs. nuclear abnormality for nuclei from cluster 1 (normal stroma) and nuclei from the evolving subpopulation (cluster 2) in ovaries of cases at high risk of developing ovarian cancer and of cases harboring a lesion.

normal nuclei seen in the surface epithelium of normal ovaries from normal-risk subjects.³ This implies that the development of epithelial inclusion cysts may represent a very early step in the chain of events that ultimately eventuates in malignancy, even in normal women with normal ovaries. Others have speculated that the lining of inclusion cysts may actually be the site of origin of ovarian cancer; our data provide support for this possibility. Of course, the alterations we report here are based on a *very* sensitive method applied to a limited number of tissue specimens. This project was designed as an exploratory, pilot undertaking to lay the scientific foundation for subsequent, larger studies, if warranted. Supervised training algorithms were used, in which diagnostic category was known to the investigator. Insufficient cases were available to form a test set for validation; that process should be accomplished in subsequent research. Therefore, our findings cannot be regarded as definitive, although they certainly are provocative. After all, the majority of ovarian malignancies develop in patients who are not considered to be at increased risk of this cancer. Thus, finding karyometric abnormalities in the

ovaries of normal-risk women with histologically normal ovaries, in a specific cellular compartment that has been previously suggested to be of particular importance in ovarian carcinogenesis, certainly warrants further inquiry.

In addition, we observed a similar, abnormal subpopulation of cells within the underlying, histologically normal appearing stroma, both in the ovaries of women with coexisting ovarian cancer and in the ovaries obtained from patients at high risk of developing ovarian cancer. Our pilot study does not allow us to determine whether these stromal changes precede those in the surface epithelium, or vice versa. However, our observations add to the growing literature¹⁷ that suggests that the stroma in tissues that have undergone malignant transformation is not simply a passive, innocent bystander. Rather, a number of experimental models have demonstrated that stromal/epithelial interactions may be at the heart of the neoplastic process.²⁰⁻²² Therefore, the stromal abnormalities detected in this study certainly merit further systematic analysis.

In summary, our data provide support for the hypothesis that the epithelia within inclusion cysts from ovaries harboring an ovarian malignancy express preneoplastic changes in the nuclear chromatin pattern. Nuclei from inclusion cyst epithelium of histologically normal ovaries obtained from women at high risk of developing ovarian cancer also express similar abnormalities. Perhaps most surprising, similar karyometric changes were also observed in the inclusion cyst epithelium of normal ovaries from normal-risk women; the ovarian surface epithelium in those women was karyometrically normal. Finally, an analogous set of abnormalities was demonstrated in the histologically normal appearing stroma from both ovaries with coexisting ovarian cancer and in ovaries obtained from high-risk women but not in normal ovaries from low-risk women. Our experience suggests that karyometric analysis of different ovarian tissue compartments may provide very useful insights into the biology and pathogenesis of ovarian cancer.

References

1. Greene MH, Clark JW, Blayney DW: The epidemiology of ovarian cancer. *Semin Oncol* 1984;11:209-226
2. Easton DF, Ford D, Bishop DT: Breast and ovarian cancer incidence in BRCA-1 mutation carriers. *Am J Hum Genet* 1995; 56:265-271
3. Brewer MA, Ranger-Moore J, Baruch A, Alberts D, Greene

- M, Thompson D, Liu Y, Davis J, Bartels P: Exploratory study of ovarian intraepithelial neoplasia. *Cancer Epidemiol Biomarkers Preven* (in press)
4. Palcic B, MacAulay C: Malignancy associated changes: Can they be employed clinically? *In* *Compendium on the Computerized Cytology and Histology Laboratory*. Edited by GL Wied, PH Bartels, D Rosenthal, U Schenck. Chicago, *Tutorials of Cytology*, 1994, pp 157-165
 5. Bartels PH, daSilva VD, Montironi R, Hamilton PW, Thompson D, Vaught L, Bartels HG: Chromatin texture signatures in nuclei from prostate lesions. *Analyt Quant Cytol Histol* 1998;20:407-416
 6. Bartels PH, Olson GB: Computer analysis of lymphocyte images. *In* *Methods of Cell Separation*. Third volume. Edited by N Catsimopoulos. New York, Plenum Press, 1980, pp 1-99
 7. McClellan RP: *Optimization and Stochastic Approximation Techniques Applied to Unsupervised Learning*. Tucson, University of Arizona, 1971
 8. Bartels PH, Thompson D, Weber JE: Unsupervised conceptual learning in a diagnostic expert system. *In* *IEEE/EMBS: 1989, 1989*, pp 1780-1781
 9. Montironi R, Scarpelli M, Mazzucchelli R, Hamilton PW, Thompson D, Ranger-Moore J, Bostwick DG, Bartels PH: Subvisual changes in chromatin organization state are detected by karyometry in the histologically normal urothelium in patients with synchronous papillary carcinoma. *Hum Pathol* 2003;34:893-901
 10. Wied GL, Bartels PH, Bibbo M, Sychra JJ: Cytomorphometric markers for uterine cancer in intermediate cells. *Analyt Quant Cytol Histol* 1980;2:257-263
 11. Bibbo M, Bartels PH, Sychra JJ, Wied GL: Chromatin appearance in intermediate cells from patients with uterine cancer. *Acta Cytol* 1981;25:23-28
 12. Bartels PH, Montironi R, Hamilton PW, Thompson D, Vaught L, Bartels HG: Nuclear chromatin texture in prostatic lesions: II. PIN and malignancy associated changes. *Analyt Quant Cytol Histol* 1998;20:397-406
 13. Susnik B, Worth A, LeRiche J, Palcic G: Malignancy associated changes in the breast: Changes in chromatin distribution in epithelial cells in normal appearing tissue adjacent to cancer. *Analyt Quant Cytol Histol* 1995;17:62-68
 14. Bibbo M, Bartels PH, Galera-Davidson H, Dytch HE, Wied GL: Markers for malignancy in the nuclear texture of histologically normal tissue from patients with thyroid tumors. *Analyt Quant Cytol Histol* 1986;8:168-176
 15. Montag AG, Bartels PH, Dytch HE, Lerma-Puertas E, Michelassi F, Bibbo M: Karyometric features in nuclei near colonic adenocarcinoma: Statistical analysis. *Analyt Quant Cytol Histol* 1991;13:159-167
 16. Beale EMI: Euclidean cluster analysis. *Bull Int Stat Inst* 1969; 43:21-43
 17. Fleiss J: *Statistical Methods for Rates and Proportions*. New York, Wiley, 1981
 18. Kruskal WH, Wallis WA: Use of ranks on one-criterion variance analysis. *J Am Stat Assoc* 1952;47:583-621, addendum, 1953;54:907-911
 19. Ip MM, Masso-Welch PA, Ip C: Prevention of mammary cancer with conjugated linoleic acid: Role of the stroma and the epithelium. *J Mammary Gland Biol Neoplasia* 2003;8:103-118
 20. Cunha GR, Hayward SW, Wang YZ, Ricke WA: Role of the stromal microenvironment in carcinogenesis of the prostate. *Int J Cancer* 2003;107:1-10
 21. Haslam SZ, Woodward TL: Host microenvironment in breast cancer development: Epithelial-cell-stromal-cell interactions and steroid hormone action in normal and cancerous mammary gland. *Breast Cancer Res* 2003;5:208-215
 22. Cunha GR, Hayward SW, Wang YZ, Ricke WA: Role of the stromal microenvironment in carcinogenesis of the prostate. *Int J Cancer* 2003;107:1-10